

SLAC-PUB-507  
November 1968  
(EXP)

PHOTOPRODUCTION OF  $\pi^- \Delta_{1236}^{++}$  FROM HYDROGEN FROM 5 TO 16 GeV\*

A. M. Boyarski, R. Diebold, S. D. Ecklund  
G. E. Fischer, Y. Murata, † B. Richter and W.S.C. Williams ‡

Stanford Linear Accelerator Center  
Stanford University, Stanford, California

ABSTRACT

Cross sections for  $\gamma p \rightarrow \pi^- \Delta_{1236}^{++}$  have been measured at 5, 8, 11 and 16 GeV from near zero momentum transfer to  $-1 \text{ GeV}^2$  ( $-2 \text{ GeV}^2$  at 16 GeV). The cross section rises from small  $t$  to a maximum near  $-t = m_\pi^2$ , then falls as  $e^{12t}$  out to  $-t \approx 0.2 \text{ GeV}^2$ , after which it becomes roughly equal in slope and magnitude to the single  $\pi^+$  photoproduction cross section ( $e^{3t}$ ). At fixed  $t$ , the cross section varies as  $k^{-2}$ , where  $k$  is the laboratory photon energy. The results do not agree well with the simple vector dominance model.

(Submitted to Phys. Rev. Letters.)

\* Work supported by the U.S. Atomic Energy Commission.

† On leave from the Institute of Nuclear Study, University of Tokyo, Japan.

‡ On leave from The Nuclear Physics Laboratory, University of Oxford, England.

The differential cross section for



has been measured at 5, 8, 11 and 16 GeV using the SLAC 20-GeV/c spectrometer system.<sup>1</sup> This work extends previous measurements in the few GeV region.<sup>2</sup>

The apparatus and method are the same as used by Boyarski *et al.*,<sup>3</sup> with two modifications. First, in addition to the Cerenkov monitor, a secondary emission quantameter (SEQ) was used to monitor the beam. Except for laboratory angles  $\lesssim 1^\circ$ , these two monitors could be used simultaneously and provided a cross check of the monitor stability; in general, this stability was found to be about  $\pm \frac{1}{2}\%$ . These monitors were calibrated against two precision calorimeters which served as absolute standards. The second change was the use of a threshold gas Cerenkov counter to separate the group  $e, \mu, \pi$  from K mesons and protons. As before, the pions were then identified by their interaction properties.

To determine the  $\Delta_{1236}^{++}$  yield, the 20-GeV/c spectrometer system was used to measure the momentum spectrum of  $\pi^-$  mesons produced in hydrogen by a bremsstrahlung beam. This yield of  $\pi^-$  mesons was determined as a function of missing mass (calculated for  $k = E_0$ , the bremsstrahlung end-point energy);  $\Delta_{1236}^{++}$  production should appear as a step in the  $\pi^-$  yield vs missing mass at  $M_X^2 = 1.53 \text{ GeV}^2$ , reflecting the step in the photon spectrum near the end point. The width of the rise of the step is mainly determined by the natural width of the  $\Delta$  with a small contribution from the experimental resolution. Data were normally taken over the range  $1.2 \leq M_X^2 \leq 2.5 \text{ GeV}^2$ .

For process (1) the shape of the  $\Delta$  was assumed to be given by a Jackson relativistic Breit-Wigner form<sup>4</sup>

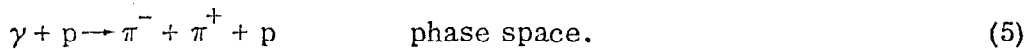
$$R(m^2) = \frac{1.13}{\pi} \frac{m_0 \Gamma(m)}{(m^2 - m_0^2)^2 + m_0^2 \Gamma^2(m)} \quad (2a)$$

with

$$\Gamma(m) = \Gamma(m_0) \left(\frac{q}{q_0}\right)^3 \left(\frac{am_{\pi}^2 + q_0^2}{am_{\pi}^2 + q^2}\right) \left(\frac{m_0}{m}\right) \quad (2b)$$

where  $m_0 = 1.236$  GeV,  $\Gamma(m_0) = 0.120$  GeV,  $a = 2.2$ ;  $q$ ,  $q_0$  are the cm momentum at mass  $m$ ,  $m_0$  in the  $\Delta$  rest system. This shape was cut off at  $m = 1.836$  GeV and the factor 1.13 normalizes the integral of  $R(m^2)$  to one. The Breit-Wigner was folded in with the bremsstrahlung spectrum (calculated for a  $0.03 X_0$  radiator<sup>5</sup>) and with the two-body  $\pi\Delta$  phase space.

Various fits were made to the  $\pi^-$  spectra assuming a contribution from reaction (1) plus a background from one or more of the processes



The contribution from  $\rho$  production [Eq. (3)] was calculated using a relativistic Breit-Wigner for the rho meson with a mass of 0.765 GeV and width 0.13 GeV; the production cross section was assumed to have a  $t$  dependence of  $e^{8t}$  and the  $\rho$  to have helicity  $\pm 1$  as indicated by experiment.<sup>6</sup> In the simple OPE model of Drell<sup>7</sup> the yield is proportional to  $\sigma_{\text{tot}}(\pi^+ p)$ ; to avoid double counting, the contribution of  $\Delta_{1236}$  was removed from the total cross section values used in the program. The background from phase space was calculated assuming a yield proportional to the available phase space only.

The fitting program did a least-squares fit to the data, varying the amount contributed by each process included in the hypothesis.<sup>8</sup> Excellent fits to the

data were obtained at all energies by attributing the background solely to  $\pi^-$ 's from  $\rho^0$  decay. Adding in other contributions to the background did not cause significant decreases in the  $\chi^2$  values, but did cause the uncertainty in the  $\Delta$  contributions to increase with corresponding random shifts in the fitted cross section. Inclusion of phase space background in the fits gave phase space contributions which were small or consistent with zero. Good fits were also obtained by attributing all the background to the Drell mechanism. At 16 GeV the  $\Delta$  cross sections obtained from the  $\Delta + \rho$  fits were almost identical to those from the  $\Delta +$  Drell fits.<sup>9</sup> Since the photoproduction of  $\rho^0$  mesons at high energies has been well established, we consider the  $\Delta + \rho$  fits to be the most reliable and have used these fits exclusively to determine the  $\Delta$  cross sections. Figure 1a shows a typical fit to the data using the hypothesis that the  $\pi^-$  yield has contributions from  $\Delta$  production,  $\rho$  production and decay, and phase space. The two background terms contribute very little to the yield in the region of the  $\Delta$  step. The least-squares fitting program usually gave statistical errors of only a few percent; we have increased these errors to a minimum of 15% to reflect our estimate of the systematic uncertainty in the background calculations. There is in addition an overall normalization uncertainty of about  $\pm 10\%$ . The  $\Delta^{++}$  differential cross sections are listed in Table I.

Figure 1b shows the differential cross section for  $\Delta$  production plotted vs  $t$ . The data at all four energies have the same general characteristics — a sharp rise from  $|t|$  of 0 to  $m_\pi^2$ , a steep fall approximately as  $e^{12t}$  from  $|t|$  of  $m_\pi^2$  to about  $0.2 \text{ GeV}^2$ , and a change in slope to about  $e^{3t}$  for  $|t| > 0.2 \text{ GeV}^2$ . For  $|t| > 0.2 \text{ GeV}^2$  the magnitude as well as the slope of the  $\Delta$  cross section is roughly the same as that found for  $\gamma p \rightarrow \pi^+ n$ . Using the Regge parametrization

$$\frac{d\sigma}{dt} = \beta(t) (s - M^2)^{2\alpha(t) - 2}, \quad (6)$$

where  $s$  is the square of the total energy in the center-of-mass system, and  $M$  is the nucleon mass, we find from the 8, 11 and 16 GeV data the values of  $\alpha$  shown in the insert in Fig. 1b. The error bars shown reflect the 15% systematic uncertainty in the cross sections. With some fluctuations, the data are consistent with  $\alpha = 0$ , i.e.,  $\Delta^{++}$  production has the same  $1/k^2$  energy dependence of the single- $\pi^\pm$  and  $K^\pm$  production cross sections.

In Fig. 1c,  $(s - M^2)^2 (d\sigma/dt)$  is plotted vs  $\sqrt{|t|}$  to better display the small momentum transfer region. The cross section rises very rapidly from  $|t|_{\min}$  to  $m_\pi^2$ , and then turns over and falls with the  $e^{12t}$  dependence characteristic of the region  $m_\pi^2 \leq |t| \leq 0.2$ . It is worth noting that when plotted in this way the results of the DESY bubble chamber are consistent with our data down to a photon energy of 1.4 GeV. We have fit all the data from  $t_{\min}$  to  $m_\pi^2$  to the form

$$(s - M^2)^2 \frac{d\sigma}{dt} = \frac{a + bt + ct^2}{(|t| + m_\pi^2)^2} \quad (7)$$

in order to extrapolate the cross section to  $t = 0$ . Equation (7) gives the  $t$  dependence to be expected from one-pion exchange plus a slowly varying background. We find

$$(s - M^2)^2 \frac{d\sigma}{dt} (t = 0) = 350 \pm 120 \mu\text{b-GeV}^2. \quad (8)$$

The solid curve in Fig. 1b shows the cross expected in a minimal, gauge-invariant extension of one-pion exchange.<sup>10</sup> This model agrees quite well with the data at very small momentum transfers and it is interesting to note that the cross sections for  $\gamma p \rightarrow \pi^+ n$ ,  $\gamma n \rightarrow \pi^- p$ , and  $\gamma p \rightarrow \pi^- \Delta^{++}$  are all reproduced to within 20% by minimal, gauge-invariant one-pion exchange over the range 5 to 16 GeV and  $|t| \lesssim 2m_\pi^2$ . At larger momentum transfers the model predicts more cross section than observed.

The total cross section for  $\Delta^{++}$  photoproduction can be obtained by integrating the forward differential cross section; the contributions from the big-t and u regions are expected to be a few percent or less. The results of this experiment give

$$\sigma(\gamma p \rightarrow \pi^- \Delta^{++}) = 33 \mu b/k^2 \quad (9)$$

(for the laboratory photon energy  $k$  in GeV) with a systematic uncertainty of  $\pm 20\%$ . This parametrization also fits the bubble chamber data,<sup>2</sup> down to  $k = 1.2$  GeV, below which there is a 50% increase near  $k = 1$  GeV and then a rapid fall-off to threshold.

The vector dominance model (VDM) has been successfully used to relate single- $\pi^\pm$  photoproduction to  $\rho^0$  production by pions.<sup>11</sup> A similar relation can be obtained for  $\Delta^{++}$  photoproduction if one assumes that

$$A(\pi^+ p \rightarrow V^0 \Delta^{++}) = A(V^0 p \rightarrow \pi^- \Delta^{++}) \quad (10)$$

Note that this assumption cannot be obtained merely by invoking time reversal and isospin invariance as was possible for the single- $\pi^\pm$  photoproduction relation, but requires in addition s-u crossing symmetry. With the above assumption VDM predicts

$$\frac{d\sigma}{dt}(\gamma p \rightarrow \pi^- \Delta^{++}) = |A_\rho + A_\omega + A_\phi|^2, \quad (11)$$

where

$$|A_V|^2 = g_{V\gamma}^2 \left[ \rho_{11}^{\text{hel}} \frac{d\sigma}{dt} \right]_{\pi^+ p \rightarrow V^0 \Delta^{++}}$$

The  $\rho$  contribution is expected to be dominant, and although  $\pi^+ p \rightarrow \rho^0 \Delta^{++}$  has been studied at low energies as well,<sup>12</sup> we will concentrate on the 8-GeV/c data of the ABC collaboration.<sup>13, 14</sup> They have obtained the  $\rho$  helicity density matrix by fitting the  $\rho$  decay angular distributions (of events with

$0.66 \leq M_{\pi^+\pi^-} \leq 0.86$  GeV and  $1.12 < M_{p\pi^+} \leq 1.32$  GeV) directly in the helicity frame. Their  $\rho_{11}^{\text{hel}}$  values are shown in the inset of Fig. 2 together with the values from lower energy experiments (obtained by rotating the density matrix from the Jackson to the helicity frame).

Using  $g_{\rho\gamma}^2 = (3.5 \pm 0.5) \times 10^{-3}$  (Ref. 15) the  $\rho$ -dominance prediction calculated from the bubble chamber data is smaller than the experimental data by roughly a factor of three, as shown in Fig. 2. To calculate the extreme limits of the vector dominance model we have assumed complete constructive (destructive) interference of the  $A_\omega$  and  $A_\rho$  amplitudes and in addition allowance for the uncertainty in the various quantities was made by adding (subtracting) one standard deviation, as calculated by adding the individual uncertainties in quadrature. The  $\omega$  differential cross section used was taken from Ref. 13,  $g_{\omega\gamma}^2 = (0.39 \pm 0.08) \times 10^{-3}$  was taken from Ref. 15, and  $\rho_{11}^\omega = 0.35 \pm 0.07$  was obtained by rotating the Jackson density matrix obtained by the ABC collaboration to the helicity frame. As can be seen from Fig. 2, the prediction and the data are just compatible for  $|t| \gtrsim 0.2$  GeV $^2$  under the extreme assumption of complete constructive interference plus a one-standard deviation shift in the parameters used to make the prediction. At  $|t| \lesssim 0.1$  GeV $^2$  there remains a factor-of-two discrepancy. Given the success of the vector dominance model for the single-pion differential cross section, we tend to ascribe the  $\Delta^{++}$  discrepancy to the assumption made in Eq. (10). This assumption is valid in general only for a single t-channel exchange and may not be valid if several t-channel exchanges are important or if factorization does not work.<sup>13</sup>

#### ACKNOWLEDGMENTS

We gratefully acknowledge the contributions of Drs. F. Bulos, W. Busza, and J. R. Rees to the design and construction of the data acquisition system. Discussions with Professor H. Harari have been most helpful.

## REFERENCES

1. Preliminary results were reported at the XIV International Conference on High Energy Physics at Vienna (1968).
2. Aachen-Berlin-Bonn-Hamburg-Heidelberg-München Collaboration, Phys. Letters 23, 707 (1966), and DESY 68/8 (May 1968); Cambridge Bubble Chamber Group, Phys. Rev. 163, 1510 (1967).
3. A. M. Boyarski, F. Bulos, W. Busza, R. Diebold, S. D. Ecklund, G. E. Fischer, J. R. Rees, and B. Richter, Phys. Rev. Letters 20, 300 (1968).
4. J. D. Jackson, Nuovo Cimento 34, 1644 (1964).
5. R. A. Early, Report No. SLAC-TN-66-15, Stanford Linear Accelerator Center, Stanford University, Stanford, California (1966).
6. Aachen-Berlin-Bonn-Hamburg-Heidelberg-München Collaboration, DESY Report 68/8 (May 1968).
7. S. D. Drell, Phys. Rev. Letters 5, 278 (1960).
8. The missing-mass scale position was varied to allow for Beam-Switch-Yard and spectrometer momentum intercalibration errors as well as for vertical beam mis-steering, which has the effect of slightly altering the central momentum of the spectrometer. The experimental resolution was found by fitting the step in the  $\pi^+$  spectrum corresponding to  $\gamma p \rightarrow \pi^+ n$ .
9. At 5 GeV the  $\Delta + \rho$  fits gave 15% to 35% less  $\Delta$  cross section than did the  $\Delta +$  Drell fits; at 8 GeV this difference was  $\lesssim 15\%$ .
10. P. Stichel and M. Scholz, Nuovo Cimento 34, 1381 (1964).
11. C. Iso and H. Yoshii, Ann Phys. 47, 424 (1968);  
A. Dar et al., Phys. Rev. Letters 20, 1261 (1968);  
M. Krammer, Phys. Letters 26B, 633 (1968); erratum 27B, 260 (1968);  
R. Diebold and J. A. Poirier, Phys. Rev. Letters 20, 1532 (1968).

12. 3-4 GeV/c: D. Brown et al., Phys. Rev. Letters 19, 664 (1967);  
4 GeV/c: ABBHLM Collaboration, quoted by N. Schmitz, CERN 65-24,  
Vol. I (Geneva, Switzerland, 1965), p. 1;  
5 GeV/c: BDPNST Collaboration, paper contributed to the 1967  
Heidelberg Conference, quoted by L. van Rossum, CERN 68-7,  
Vol. I (Geneva, Switzerland, 1968), p. 161.
13. Aachen-Berlin-CERN Collaboration, Phys. Letters 27B, 174 (1968); and  
preprint to be submitted to Nuclear Physics.
14. D. R. O. Morrison, private communication.
15. S. C. C. Ting, rapporteur talk at the XIV International Conference on High  
Energy Physics, Vienna (1968).

TABLE I  
DIFFERENTIAL CROSS SECTIONS FOR  $\gamma + p \rightarrow \pi^- + \Delta^{++}$

5 GeV		8 GeV		11 GeV		16 GeV	
$-t_{\min} = 0.00148 \text{ GeV}^2$	$-t_{\min} = 0.00090 \text{ GeV}^2$	$-t_{\min} = 0.00063 \text{ GeV}^2$	$-t_{\min} = 0.00043 \text{ GeV}^2$	$-t$ $\text{GeV}^2$	$\frac{d\sigma}{dt}$ $\mu\text{b}/\text{GeV}^2$	$-t$ $\text{GeV}^2$	$\frac{d\sigma}{dt}$ $\mu\text{b}/\text{GeV}^2$
0.0017	< 12	0.00106	$2.18 \pm 0.75$	0.00093	$1.81 \pm 0.27$	0.00097	$0.596 \pm 0.089$
0.0050	$10.2 \pm 1.5$	0.00145	$2.94 \pm 0.79$	0.00164	$1.30 \pm 0.20$	0.00261	$0.809 \pm 0.122$
0.0101	$10.9 \pm 1.6$	0.00351	$3.62 \pm 0.58$	0.00380	$2.70 \pm 0.40$	0.00971	$0.982 \pm 0.133$
0.0201	$10.7 \pm 1.6$	0.00431	$4.31 \pm 0.65$	0.00582	$2.54 \pm 0.38$	0.0134	$1.16 \pm 0.17$
0.0399	$7.90 \pm 1.2$	0.00521	$4.26 \pm 0.68$	0.00836	$2.18 \pm 0.33$	0.0176	$1.05 \pm 0.16$
0.0701	$5.77 \pm 0.86$	0.00620	$4.51 \pm 0.68$	0.0114	$1.83 \pm 0.27$	0.0212	$0.900 \pm 0.135$
0.150	$2.64 \pm 0.40$	0.0101	$4.33 \pm 0.65$	0.0201	$2.10 \pm 0.31$	0.0396	$0.682 \pm 0.102$
0.250	$1.14 \pm 0.17$	0.0198	$4.33 \pm 0.65$	0.0400	$1.69 \pm 0.25$	0.0694	$0.486 \pm 0.073$
0.400	$0.478 \pm 0.072$	0.0376	$3.71 \pm 0.56$	0.0705	$1.19 \pm 0.18$	0.0991	$0.326 \pm 0.049$
0.600	$0.280 \pm 0.042$	0.0688	$2.14 \pm 0.32$	0.150	$0.459 \pm 0.069$	0.149	$0.182 \pm 0.027$
		0.152	$1.05 \pm 0.16$	0.249	$0.226 \pm 0.033$	0.249	$0.0968 \pm 0.0150$
		0.246	$0.479 \pm 0.072$	0.400	$0.107 \pm 0.016$	0.399	$0.0657 \pm 0.0100$
		0.401	$0.237 \pm 0.036$	0.601	$0.0812 \pm 0.0122$	0.597	$0.0472 \pm 0.0072$
		0.602	$0.113 \pm 0.017$	1.00	$0.0351 \pm 0.0053$	0.796	$0.0283 \pm 0.0042$
		0.801	$0.104 \pm 0.016$			0.999	$0.0170 \pm 0.0025$
		1.035	$0.068 \pm 0.010$			1.50	$0.00255 \pm 0.00038$
						2.00	$0.00035 \pm 0.00009$

### FIGURE CAPTIONS

1. (a) Fit to the  $\pi^-$  yield. Solid curves give the individual contributions, and the dashed curve is the sum of the solid curves.  
(b) Differential cross section vs momentum transfer. The dashed lines are smooth curves through the single- $\pi^+$  photoproduction data of Ref. 3. The insert shows the Regge parameter  $\alpha$  vs  $t$ .  
(c) The small- $t$  cross section on an expanded scale. The curve is the gauge-invariant OPE calculation of Ref. 10.
2. Comparison of photoproduction of  $\pi^-\Delta^{++}$  and pion production of  $\rho^0\Delta^{++}$  and  $\omega^0\Delta^{++}$  by means of the vector dominance model. The crosses represent the  $\rho^0$  contribution. The boundaries of the cross-hatched region give the limits of the  $\rho$  plus  $\omega$  contribution assuming maximum  $\rho - \omega$  interference and including the statistical plus systematic errors added in quadrature. The solid points are the results of this experiment at 8 GeV. The insert shows  $\rho_{11}$  (helicity) used to determine the  $\rho\Delta^{++}$  contribution.

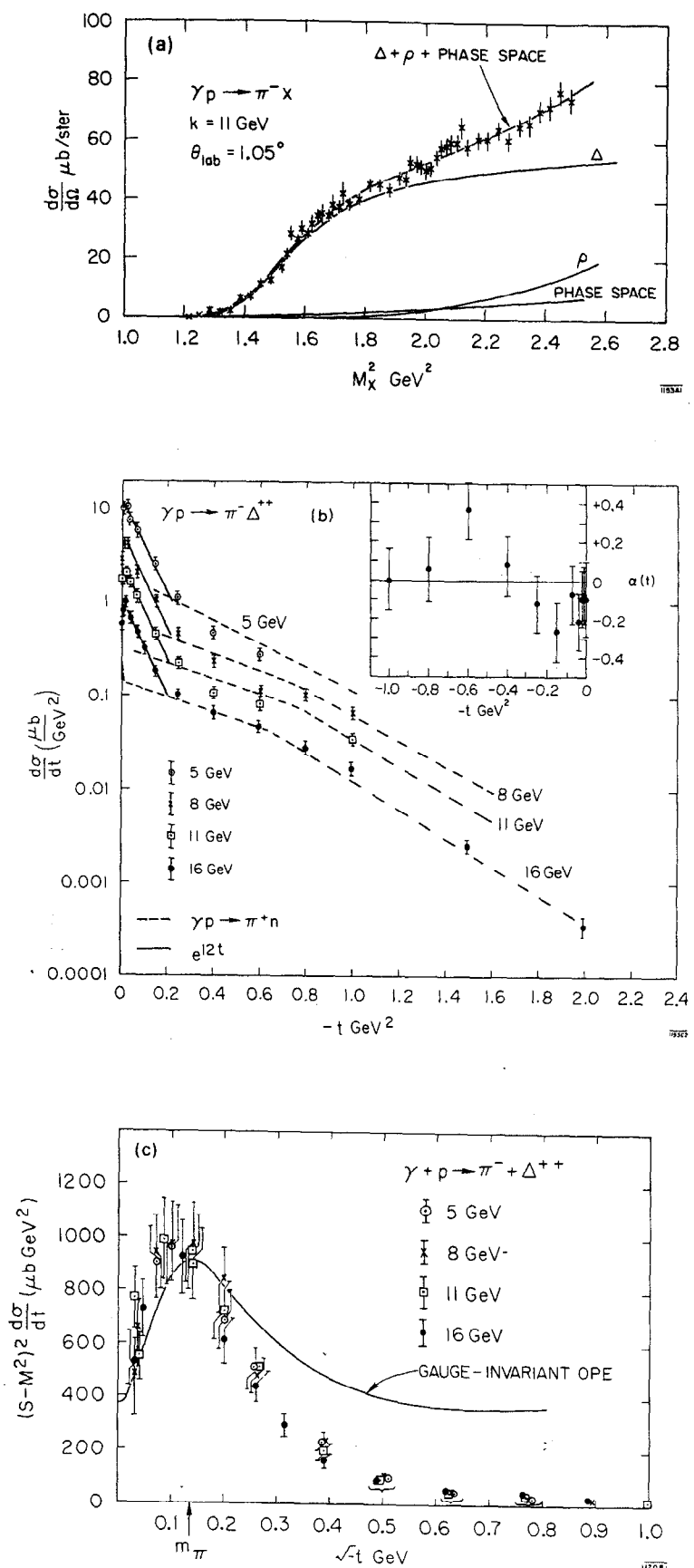


Fig. 1

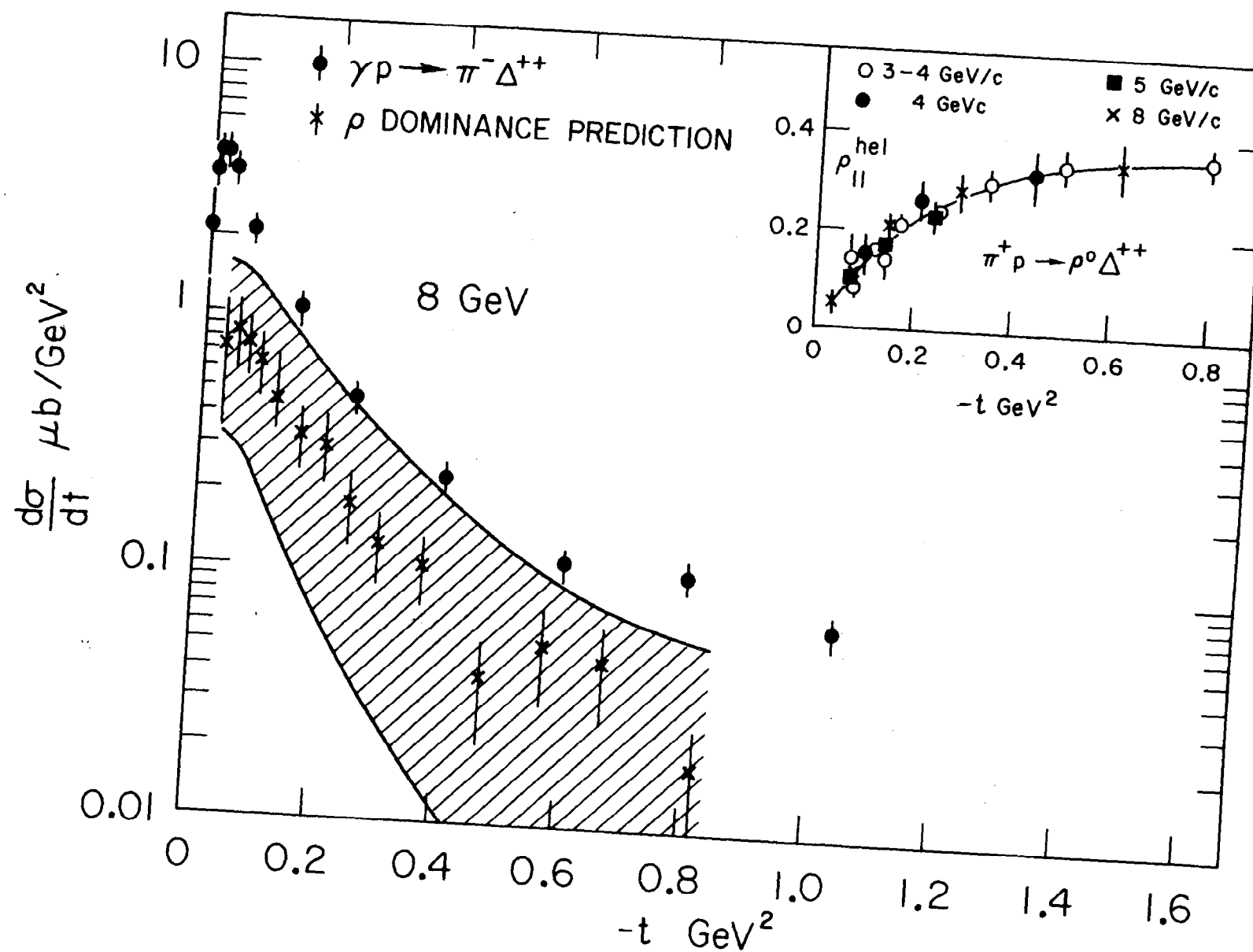


Fig. 2

115383